TAO, Vol. 9, No. 4, 573-588, December 1998

A Preliminary Study on Crustal Anisotropy in Chia-Nan Area of Taiwan

Chau Huei Chen[1] and Huei Jeng Yen[1]

(Manuscript received 17 December 1997, in final form 11 May 1998)

ABSTRACT

Twenty nine events recorded at three stations in the Chia-Nan area of Taiwan showed split S waveforms with delay times ranging between 0.1 and 0.2 s. Aspect ratio method was applied to retrieve anisotropic properties of these phases. Data at station CHY were characterized by roughly E-W fast direction that is parallel or sub-parallel to the compressional axis in the region, as determined by other approaches. Stations ALS and SGS recorded split waveforms that showed fast directions oblique with respect to the apparent regional compressional axis, but sub-parallel to that of the orientation of the secondary faults in the vicinity. To verify the anisotropic nature of splitting, 6 events were selected to construct polarization patterns in which splitting was removed. The observed splitting-corrected polarizations agreed with those given by reliably determined focal mechanisms of these events, therefore excluding extrinsic contributions from the sources. Analyses from ALS and SGS indicated that seismic anisotropy observed at local and regional scales may not be fully accounted for by the Extensive Dilatancy Anisotropyc (EDA) theory but rather are controlled by conditions in the local fault system.

(Key words: Crustal, Anisotroty)

1. INTRODUCTION

Seismic anisotropy on the upper crust may be generated by stress-induced parallel microcracks striking in the direction of the maximum compression and perpendicular to the minimum compression (Kehle, 1964; Atkinson, 1984; Crampin, 1987). Recently, many researchers have studied local earthquakes using closely-spaced, three-components networks to investigate shear wave splitting due to the dilatancy-induced anisotropy (*e.g.*, Booth *et al.*, 1985; Crampin and Booth, 1985; Kaneshima *et al.*, 1987; Kaneshima and Ando, 1989). The leading and following shear waves have been explained as 2 phases split from an initally unipolarized S when propagated through an anisotropic crust with small parallel tensional cracks resulting from tectonic compression between seismic stations and earthquake foci (Crampin,

[1]Institute of Seismology, National Chung Cheng University, Chia-Yi, Taiwan, ROC

1978; Crampin *et al.*, 1984). As a result, the polarization direction of the leading shear wave is nearly parallel to the direction of the maximum horizontal compressive stress. On the other hand, as shown in some research reports (Peacock *et al.*, 1988; Kaneshima and Ando, 1989; Gledhill, 1991; Zuniga *et al.*, 1995), the observed polarization directions of the leading shear wave just reflect the local crack aligment near the recording site. This implies that the direction of the maximum horizontal compressive stress from shear-wave splitting analysis may not represent the direction of the actual regional tectonic stress.

The island of Taiwan is thought to have been created by the impingement of an island-arc on the edge of the Asian continent. Because of this, compressive tectonism built a systematic structure in Taiwan. The seismicity and field surveys show that the building mechanism is still active even today. In this study, we explore the orientation of the dominant stress that affects regional structures in the Chia-Nan area by analyzing the polarization directions of the leading shear waves of the split S waves. The underlying assumption is that the anisotropy is crack-induced mainly in the upper crust, rather than being caused by preferred orientation of mineral crystals, which is usually invoked to explain large scale anisotropy in the upper mantle (Christensen, 1984; Montagner and Tanimoto, 1990; Savage and Silver, 1990).

29 events detected at 3 stations (Figure 1) showed significantly anomalous waveforms; they were at CHY, ALS, and SGS of the Central Weather Bureau Seismic Network (CWBSN), which was upgraded to digital recording in 1990. The triggered seismographs recorded ground velocity in three orthogonal directions (north-east, east-west and vertical) with a sampling rate of 100 Hz and a natural frequency of 1 Hz. All events were within the shear window of the respective stations, being about 35° (Nuttli, 1963). This angle corresponded to the critical incident angle of S-to-P conversion, that is, for Vp/Vs=1.7 (Booth and Crampin, 1985). This constraint can reduce the contamination from the distortion of a direct S phase associated with a conversion.

2. METHOD

The aspect ratio method (Shih *et al.*, 1989; 1991) provides a procedure for evaluating the linearity of the particle motion by its aspect ratio, which is the ratio of two projected particle displacements along a pair of orthogonal axes. The detailed procedure of used in this method to determine the polarization direction and the delay time between split shear waves are as follows:

For a wave propagating along the z-axis, or the vertical axis, the particle displacements of the shear wave, u_x and u_y in x and y direction can be described as the following equation (1) (Bullen and Bolt, 1985; Shih *et al.*, 1989):

$$\frac{u_x^2}{A_x^2}+\frac{u_y^2}{A_y^2}-\frac{2u_xu_y}{A_xA_y}\cos\left(\xi_y-\xi_x\right)=\sin^2\left(\xi_y-\xi_x\right) \qquad (1)$$

where A_i and ξ_i (i=x,y) represent the amplitude and the phase respectively. Particle motion is generally elliptical in nature, but the motion becomes linearly polarized when (a) there is only one shear wave (i. e., A_x or A_y is zero) or (b) there are two shear waves and the phase

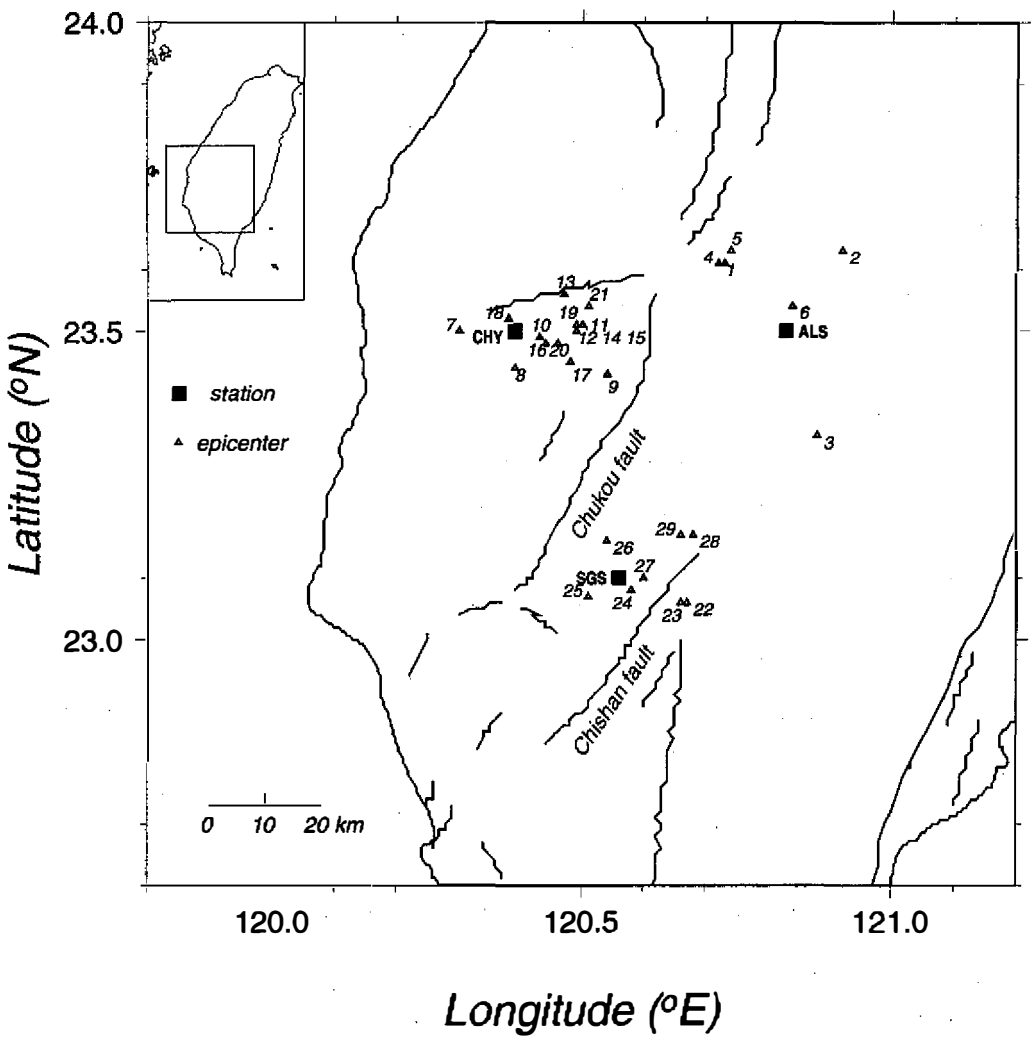

Fig. 1. The distribution of stations (solid square) where the records of the ground velocity which are used in this study. The epicenters of the triggered earthquakes are also shown (triangle). The solid curves represent the surface fault traces.

difference between them is n π , and n is an integer. The polarization of the fast shear wave is determined under the condition (a) and the time window is chosen in such a way that it includes the earliest shear-wave arrival only. The sums (D_x^* , D_y^*) of the absolute values of the projected particle displacements on a pair of orthogonal axes, x^* and y^* are then calculated.

The aspect ratio of a particle motion is defined as,

$$\frac{D^*_{x_j}}{D^*_{y_j}} = \frac{\sum_{i=1}^{n-1} d_i \left|\cos\left(\theta_j - e_i\right)\right|}{\sum_{i=1}^{n-1} d_i \left|\sin\left(\theta_j - e_i\right)\right|} \tag{2}$$

In which

$$e_i = \tan^{-1}\frac{\left(y_i - y_{i+1}\right)}{\left(x_i - x_{i+1}\right)}$$

and

$$d_i = \sqrt{\left(y_i - y_{i+1}\right)^2 + \left(x_i - x_{i+1}\right)^2}$$

where d_j are the samples of two orthogonal velocity time series. In addition, n is the total number of samples with an equal time step, θ_j is the rotation angle of the new coodinate, and j is the index of the angle increment. A nearly linear particle motion, which can be infered from the maximun value of the aspect ratio, occurs when the projection direction is nearly parallel to the major axes of the chosen coordinates. Therefore, the polarization direction of the fast shear wave can be determined objectively (Gledhill, 1991):

$$\text{Polarization Direction} = R \pm \tan^{-1}(1/\text{Amax}), \tag{3}$$

where R is the angle of rotation with the largest aspect ratio, Amax.

Based on condition (b) of linear polarization, time separation is determined by maximizing the aspect ratio as a function of time lag. The time lag corresponding to the maximum aspect ratio value is the separation time between the two splitted shear waves. In this case, the phase difference between the two shear waves is either 0 or π.

3. ANALYSIS

3.1 Incident Angle

The particle motions of shear wave arrivals must be examined to assure that (1) the arrivals lie within the shear wave window, that is, they are not seriously contaminated by S-P conversions, and (2) they meet the prerequisite conditions of the aspect ratio method which assumes that the S-wave propagates along the vertical axis. In other words, the particle motion determined from the two horizontal components can describe the shear wave polarization adequately. If the incident angle of a shear wave is greater than the critical angle [*i.e.*, $\sin^{-1}(v_s/$

v_p)], a simple S pulse can hardly be recognized in both waveform and polarization at the surface interface, due to the effect of mode conversion (Crampin and Booth, 1985). Only when the incident angle is less than the critical one, can the splitting of an incident shear wave be easily recognized from surface observations. The shear window apparently determined by event-receiver geometry may be overestimated due to ignorance of lateral heterogeneity and complicated structures of the crust. In order to guarantee that the incident angles of our sample data fall into the shear wave window, apparent incident angles were measured by maximizing the aspect ratio between the vertical (V) and the radial (R) components in the time window that included the direct P arrival. This measurement procedure was performed by rotating two horizontal components to the radial (R) and the tangential (T) components, then calculating the values of the aspect ratio between V and R components for various rotation angles about the T axis. The rotation angle with the maximum aspect ratio thus approximates the real incident angle of P (Figure 2(a)). In this way, the surface perpendicular to the P incidence could be found, and the new orthogonal system, which is attached to the coming ray, could be constructed. The original R and V axes were rotated to the new Y and X axes, and the T axis remained unchanged. The shear-wave splitting analysis was carried on with the waveforms on the Y and T directions in this new ray coordinates.

The advantage of using the ray coordinates can be illustrated by the following example. Figure 2(b) shows that the P energy has been eliminated from the Y and T components on the ray-perpendicular plane, while there is energy on the Y component suspected to have been caused by P to S conversion. This result implies that the incident angle can be measured with confidence. Although the procedure applies to P, we assume that P and S waves travel along the same path with a constant Poisson ratio 0.25. We are confident that the determination of shear wave window in this study is less uncertain than determinations made by the traditional, event-receiver geometry method.

3.2 Polarization Direction and Splitting Time

To determine the polarization direction of the leading shear wave and the delay time, the aspect ratio has to be executed with a time window ideally covering the fast phase only. The aspect ratio is calculated in this time window for various azimuths, and the maximum value will correspond to the polarization direction of the fast shear wave (Figure 3a). Sometimes the size of a suitable time window can be determined visually by rotating a seismogram. In this study, we adopted the more objective multiple aspect-ratio calculation procedure advocated by Shih *et al.*, 1989 to determine the size of the window. This procedure starts from a small time window (*e.g.*, 0.05 s) with successively increasing widths until the polarity of the fast shear wave becomes unstable, that is, the aspect ratio begins to oscillate or diverge irregularly. The aspect ratio method can also be used to estimate the separation time between two splitting shear waves. After the horizontal components are rotated to the polarization directions of fast and slow shear waves, the slow shear wave arrival is advanced by small time steps (0.01 second in this study) and the aspect-ratio values are re-calculated recursively. In this case, the aspect ratio is a function of time shift taken rather than azimuth, and the maximum of the function thus indicates the delay time between the two splitting phases according to (b) (Fig-

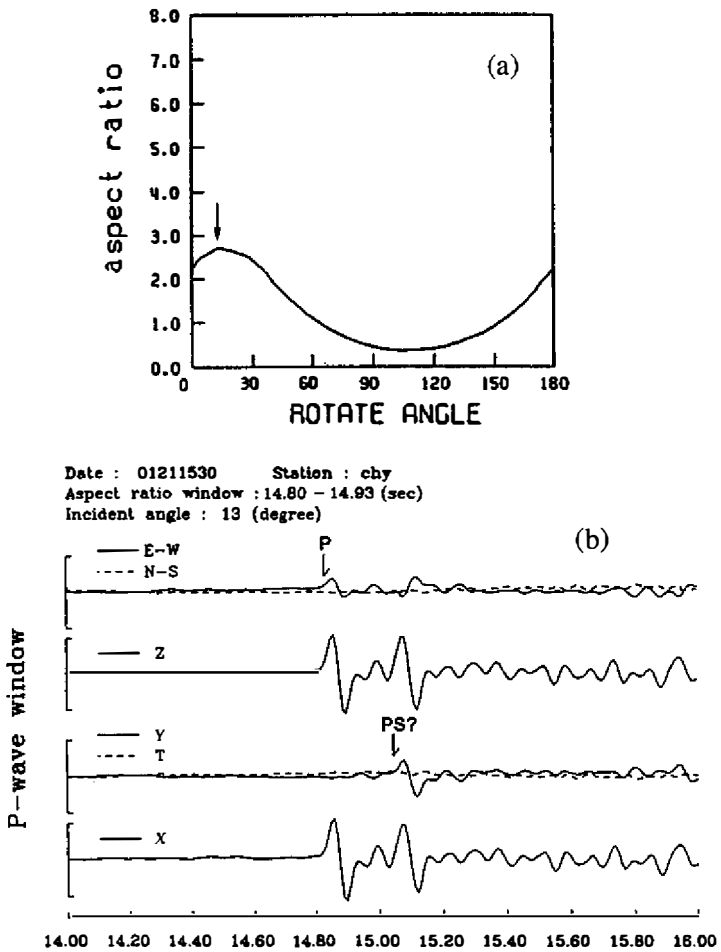

Fig. 2. (a) The example of the variation of aspect ratio versus rotation angle for the vertical and radial components. The angle with the maximum aspect ratio corresponds the incidence angle. (b) The original seismograms (E-W, N-S and Z components) and the rotated records according to the estimated incidence angle (Y, T and X components).

ure 3b). Figure 3c shows an example of the various products of the analysis procedure described above.

4. RESULTS AND DISCUSSION

4.1 Focal Mechanisms and Shear Wave Polarization

In an isotropic medium, shear wave polarization recorded at a seismograph station should reflect the source mechanism of the earthquake, as long as the waveform is not seriously distorted by scatters (Evans, 1984). If a single, uniformly anisotropic layer between the source and the station exists, the polorization pattern no longer reflects the source but is dictated by splitting caused by anisotropy. Once the splitting parameters are determined accurately, one can, however, remove this effect of the waveforms and, presumably, recover the pattern of polarization of the source. To do this, we closed the gap between the fast and slow phases and

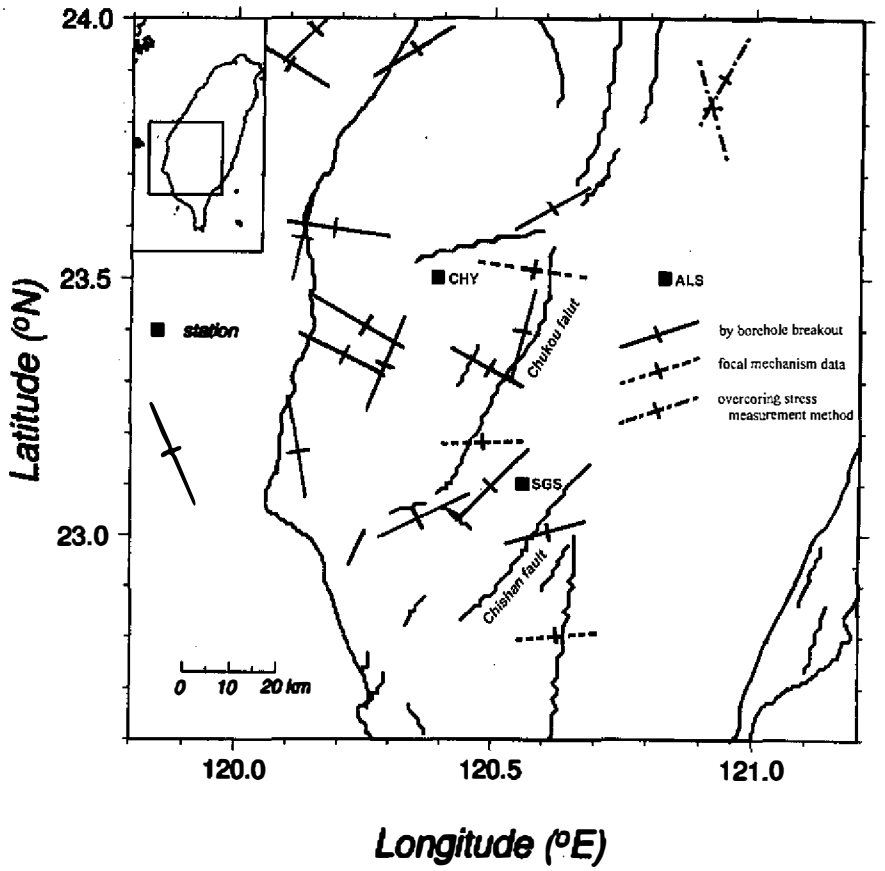

Fig. 6. The compiled local stress directions obtained from various methods.

sites (Gledhill, 1991). The conflicting results of Shih and Meyer (1990) and Savage *et al.* (1990) in Long Valley Caldera, California, can also be explained if it is assumed that both pervasive EDA anisotropy and near-surface structural anisotropy are present (Gledhill, 1991). Zuniga *et al.* (1995) also indicated that faults and fractures aligned obliquely to the main tectonic trend have a greater influence on the anisotropic characteristics than that of the regional stress field. That the polarization directions of fast S wave are roughly parallel to the direction of the regional compressive stress or the strikes of faults near stations in this area can be due to the local structure influence. Figure 6 shows the compiled results of various studies for stress direction (Lee and Chu, 1991) in the study area. The roughly E-W stress direction obtained from seismic focal mechanism and GPS surveys (Yu and Chen, 1998) indicated the present tectonic stress field. The other conflict stress directions obtained from borehole measurements and surface geological observations have been explained in terms of temporal variation of tectonic stress field during geological evolution (Lee and Chu, 1991). These results are consistent with those obtained from ALS and SGS. This implies that the micro-cracks result-

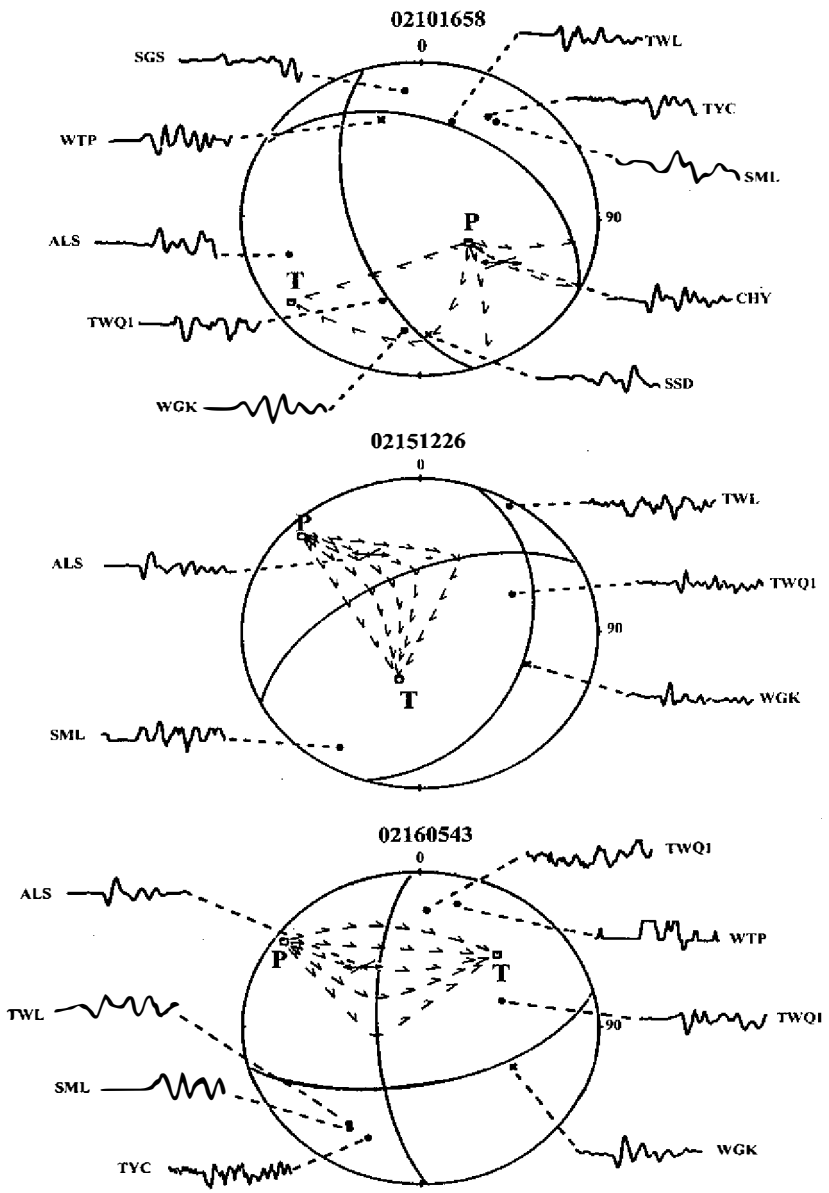

Fig. 4. The focal mechanisms derived from the first motions of the P wave and the predicted polarization directions of the shear waves (single-head arrows). The observed polarization directions of the shear waves (dot double-head arrows) are not consistent with the predicted directions, but obvious improvements are obtained after the correction (double-head arrows) according to shear wave splitting analysis.

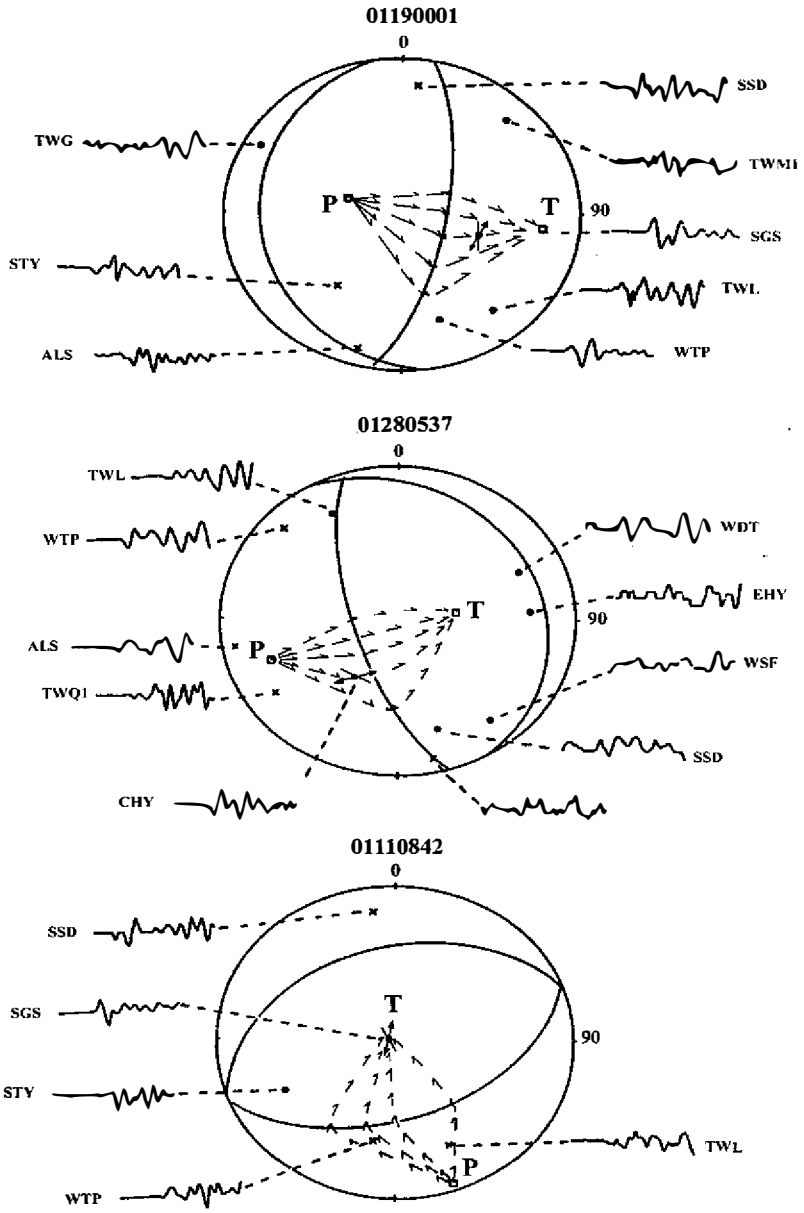

(*Fig. 4.* continued)

rotated the seismograms back to the original azimuth. The corrected shear wave polarization pattern was then compared with the pattern predicted from one the focal mechanism of that particular source. In this study, we were able to obtain reliable double-coupled focal mechanisms for only six events using P first motions (Figure 4). For these six events, the observed,

corrected polarization patterns were in reasonable agreement with those derived from focal mechanisms. The above comparison ruled out the possibility in which the observed anomalous waveforms of these 6 events are due to anomalous source mechanism rather than propagation effects. This also strengthened the argument that the split waveforms were a product of anisotropy.

4.2 Polarization Direction and Splitting Time

We obtained different directions of fast shear wave and splitting times for the three stations (Figures 5). At station CHY, which is underlain by thick, recent sediments, the average of fast-S directions derived from 15 records (Figure 5a) were aligned roughly along the E-W direction and perpendicular to the nearby segment of Chaochu Fault (Figure 1), which was consistent with the compressional axis direction suggested by previous studies. The agreement between the fast direction and regional compressional axis is in accord with the EDA

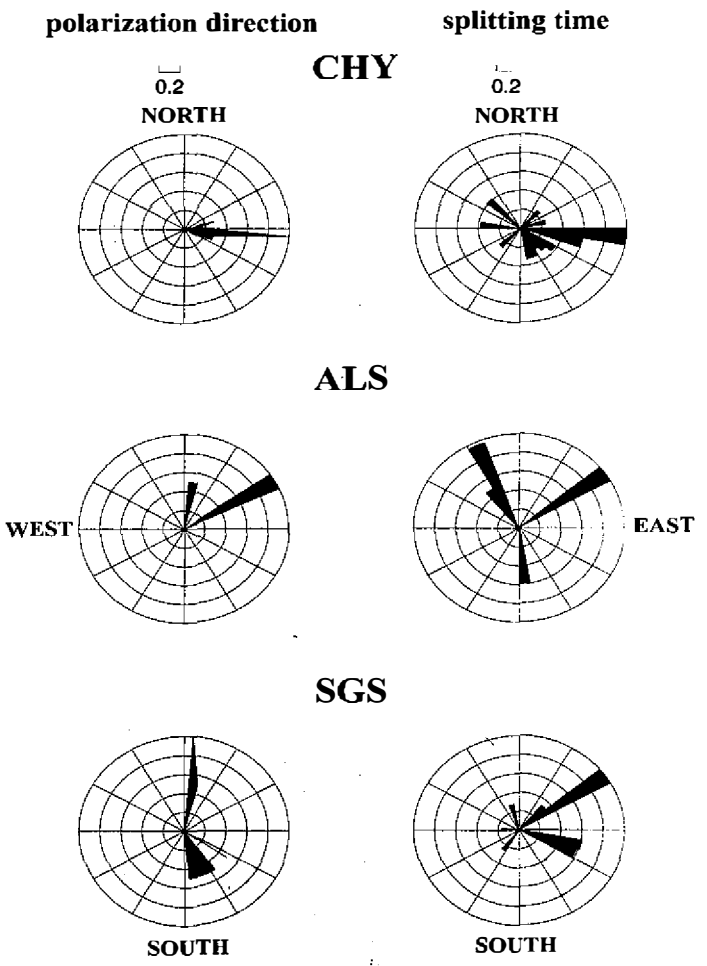

Fig. 5. The rose diagrams of the polarization direction (left column) and the splitting time (right column) for station CHY, ALS and SGS. The number of events for each azimuth range is normalized to the largest one.

hypothesis advocated by Crampin *et al.* (1984) which states that stress induced cracks filled with intergranular fluid tend to align with the maximum compression and pop up in the least compressional directions. A previous microearthquake study (Chen, 1993) also showed that the regional stress field in the Chia-Nan area is dominated by nearly E-W compressional stress. The shear wave polarization alignments measured in station CHY agreed well with both this stress direction and the result obtained from other geological studies (Chu and Lee, 1991). The EDA hypothesis is, therefore, one answer for the anisotropy observed in station CHY.

The average delay time for CHY is 0.133 sec, which was roughly dependent on the event-receiver azimuth. According to theoretical calculations (Crampin and McGonigle, 1981; Crampin and Booth, 1985; Peacock *et al.*, 1988; Kaneshima and Ando, 1989), a long delay time occurs when the ray paths are parallel to the crack surface. For station CHY, the longest and shortest delay times occur with the ray paths are roughly parallel and perpendicular to the direction of the fast S-wave polarization, respectively. To estimate how thick this layer could be, we compared the magnitude of variation in observed delay times (0.08 s) with the theoretical value (see Crampin and Booth, 1985 for details). The estimated thicknesses were about 2 and 3 km for dry and saturated parallel cracks, respectively.

Although only six seismograms from station ALS were analyzed, the average polarization direction of the fast shear waves derived from records of this station was N61°E$\pm$15°. In which, there are anomalies from 2 events. The polarization directions of these 2 events showed a nearly N-S direction and is similar to that derived from records of station SGS, which will be discussed later. The fast S wave direction derived from ALS was not consistent with that obtained at CHY, but it was consistent with the results from borehole measurements (Lee and Chu, 1991). The time lags (Figure 5d) between the fast and slow shear waves seemed dependent on the event-receiver azimuth as CHY and are within the same range as that of station CHY. Because there were not enough data, we could not obtain other information.

The polarization directions of fast shear waves recorded at station SGS can be separated into two groups: N25°W$\pm$12° (3 events) and N4°E$\pm$17° (5 events). These two directions can be considered as a nearly N-S direction (Figure 1). Nevertheless, the direction is parallel to the linear pattern of fault traces in southwestern Taiwan and the borehole measurements (Lee and Chu, 1991). The time lags between the fast and slow shear waves obtained from this station fall into a wider range than those obtained from stations CHY and ALS.

It has been noted that large variations in polarization may occur in the adjacent stations (Peacock *et al.*, 1988; Kaneshima and Ando,1989; Gledhill, 1991; Zuniga *et al.*, 1995). To confirm the significance of such variations, the effect of topography should be considered first. The topography and near-surface layers may cause scattering and reverberation, which reduce the effective signal-to-noise ratio of shear wave arrivals, and they will cause a large uncertainty of polarization direction. For a gentle slope (<10°) near the receiver, such as the stations in this study, near surface effect can be ignored (Crampin, personal communication). The field geological information near these stations, mentioned above, inclined us to ignore the topography effect in this study. So, there are several possible explanations of the observed pattern of the alignments of shear wave polarization. It is likely that the observed polarization alignments just reflect the relatively near-surface (2-3 km) structures around the recording

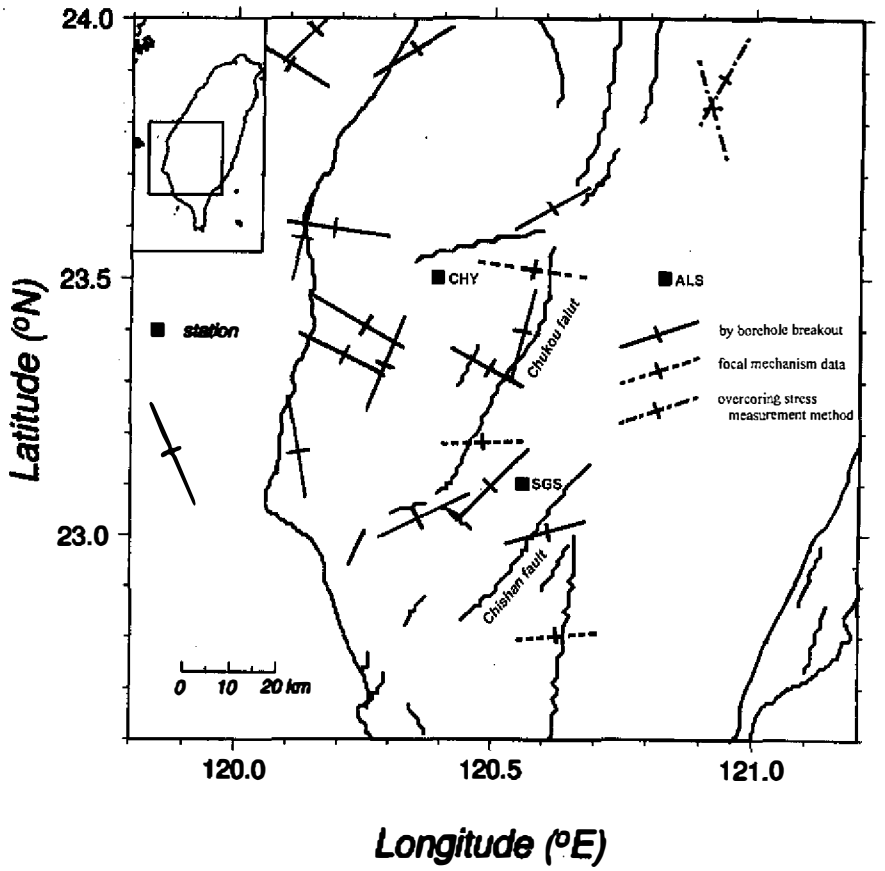

Fig. 6. The compiled local stress directions obtained from various methods.

sites (Gledhill, 1991). The conflicting results of Shih and Meyer (1990) and Savage *et al.* (1990) in Long Valley Caldera, California, can also be explained if it is assumed that both pervasive EDA anisotropy and near-surface structural anisotropy are present (Gledhill, 1991). Zuniga *et al.* (1995) also indicated that faults and fractures aligned obliquely to the main tectonic trend have a greater influence on the anisotropic characteristics than that of the regional stress field. That the polarization directions of fast S wave are roughly parallel to the direction of the regional compressive stress or the strikes of faults near stations in this area can be due to the local structure influence. Figure 6 shows the compiled results of various studies for stress direction (Lee and Chu, 1991) in the study area. The roughly E-W stress direction obtained from seismic focal mechanism and GPS surveys (Yu and Chen, 1998) indicated the present tectonic stress field. The other conflict stress directions obtained from borehole measurements and surface geological observations have been explained in terms of temporal variation of tectonic stress field during geological evolution (Lee and Chu, 1991). These results are consistent with those obtained from ALS and SGS. This implies that the micro-cracks result-

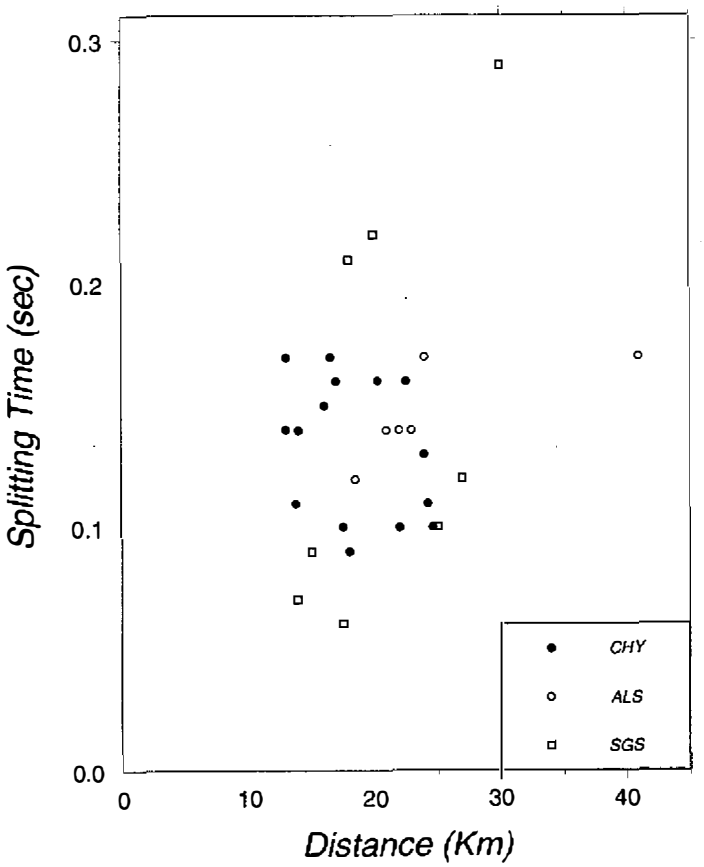

Fig. 7. The distribution of the splitting times for different ray travel distances. It shows that the splitting time is independent to the travel distance for all stations.

ing from tectonic stress fields of different geological stages could be "frozen" in corresponding geological formations beneath the station (Figure 1) and revealed by the polarization directions of the fast S-wave. Nevertheless, it also has been noted that the splitting time is independent on the travel distances of rays (Figure 7). This indicates that all ray paths share the same source of anisotropy. Considering the nearly vertical ray paths, we infered that the depth of the anisotropic layer(s) would not be larger than the focal depth of the shallowest event used in this study (*e.g.*, 10 km). These varies evidences made us believe that the large station-to-station variations of the direction of shear wave polarization could be caused by the nature of near-surface cracks in this area.

5. CONCLUSION

This preliminary study on crustal anisotropy focuses on shear wave splitting observed in a number of seismograms recorded at the seismic stations in the Chia-Nan area of Taiwan. After a simple correction for the shear wave splitting, the observed polarization and the expected ones calculated from a double-couple focal mechanism were found to be in good agreement. This implied the existence of seismic anisotropy in this area.

At the CHY station, the observed polarization directions of the faster shear waves indicated that the shear wave splitting due to seismic anisotropy may be caused by a set of vertical microcracks striking at the nearly E-W direction. The estimated strike of cracks is coincident with the direction of the tectonic stress within the upper crust, and it is inferred from the composite focal mechanism analysis of micro-earthquakes. This observation suggested that the cracks were induced by the tectonic stress (EDA hypothesis). On the other hand, large station-to-station variations in the observed shear wave polarization were also observed. In addition, the directions of these polarizations were roughly parallel to the directions of local stress derived from near-surface cracks. This may reflect that local shallow crustal structures (the nature of faulted blocks) have great influence on the polarization direction of the shear waves splitting. Our results show that both pervasive and near-surface anisotropy with different characteristics are observed in the Chia-Nan area, and this implies that the EDA hypothesis cannot explain all the phenomena of crustal anisotropy in that area.

Quantitative analyses of differential travel times between the fast and slow splitted shear waves suggest that seismic anisotropy may be concentrated in a thin surface layer. Most of the splitting times fell in the range of 0.1 to 0.2 sec. Although in this study we do not have a good velocity model to estimate the effect of velocity anisotropy in the upper crust, the short travel distance of a shear wave with a large separated time still implies a strong velocity anisotropy in this area. To understand the significance in geological structure of subsurface anisotropic velocity distribution in this area, we will conduct forward modeling of anisotropic velocity structure in the near future.

Acknowledgments The authors thank Prof. B. Y. Kuo, W. H. Wang and Y. S. Ma for useful suggestions and comments to improve this work. This study was partly supported by the National Sciences Council of the R.O.C., under Grant NSC-87-2119-M-194-004.

REFERENCES

Ando, M., Y. Ishikawa, and F. Yamazaki, 1983: Shear-wave polarization anisotropy in upper mantle beneath Honshu, Japan. *J. Geophys. Res.*, **88**, 5850-5864.

Atkinson, B. K., 1984: Subcritical crack growth in geological materials. *J. Geophys. Res.*, **89**, 4077-4114,.

Booth, D. C., S. Crampin, R. Evans, and G. Roberts, 1985: Shear-wave polarization near the north Anatolian Fault, I, Evidence for anisotropy-induced shear-wave splitting. *Geophys. J., R. Astron. Soc.*, **83**, 61-73.

Bowman, R. J., and M. Ando, 1987: Shear splitting in the upper-mantle wedge above the Tonga subduction zone. Geophys. *J. ,R. Astron. Soc.*, **88**, 25-41.

Bullen, K. E., and B. A. Bolt, 1985: An introduction to the theory of seismology. New York.

Chen, C. H., 1993: The composite fault plane solution of the Chia-Nan area, Taiwan. Report of CWB, R.O.C.

Christensen, N. I., 1984: The magnitude, symmetry and origin of upper mantle anisotropy based on fabric analyses of ultramafic tectonites, Geo phys. *J. R. Astron. Soc.*,**76**, 89-

111.

Crampin, S., 1978: Seismic wave propagation through a crack solid: Polarization as a possible diagnostic. Geophys. *J. R. Astron. Soc.*, **53**, 467-469.

Crampin, S., 1987: Geological and industrial implications of extensive-dilatancy anisotropy, *Nature*, **328**, 491-496.

Crampin, S., and R. McGonigle, 1981: The variation of delay in stress-induced anisotropic polarization anomalies. Geophys. *J. R. Astron. Soc.*, **64**, 15-31.

Crampin, S., E. M. Chesnokov, and R.G. Aipkin, 1984: Seismic anisotropy : The state of the art. Geophys. *J. R. Astron. Soc.*, **76**, 1-16.

Crampin, S., and D. C. Booth, 1985: Shear-wave polarization near the north Anatolian Fault, II, Interpretation in terms of crack-induced anisotropy. Geophys. *J. R. Astron. Soc.*, **83**, 75-92.

Crampin, S., Evans, R., and Ucer, S. B., 1985: Analysis of records local earthquakes : The Turkish dilatancy Projects (TDP1 and TDP2). Geophys. *J. R. Astron. Soc.*, **83**, 1-16.

Evans, R., 1984: Effects of the free surface on shear wavetrains. Geophys. *J. R. Astron. Soc.*, **76**, 165-172.

Gledhill, K. R., 1991: Evidence for shallow and pervasive seismic anisotropic in the Wellington region, New Zealand. *J. Geophys. Res.*, **96**, 21503-21516.

Kaneshima, S., M. Ando, and S. Crampin, 1987: Shear-wave splitting above small earthquakes in the Kinki district of Japan. *Phys. Earth Planet. Inter.*, **45**, 45-58.

Kaneshima, S., M. Ando, 1989: An analysis of split shear wave observed above crustal and uppermost mantle earthquakes beneath Shikoku, Japan: Implications in effective depth extent of seismic anisotropy. *J. Geophys. Res.*, **94**, 14077-14092.

Kehle, K. O., 1964: The determination of tectonic stresses through analysis of hydraulic well fracturing. *J. Geophys. Res.*, **69**, 259-272.

Lee, C. T., and H. T. Chu, 1991: The distribution of the Plio-Quaternary Arc-continent collision in Taiwan, Taicrust Workshop Proceedings, June 10-12, 77-81.

Montagner, J.-P., and T. Tanimoto, 1990: Global anisotropy in the upper mantle inferred from the regionalization of phase velocity, *J. Geophys. Res.*, **95**, 4797-4819.

Nuttli, O., 1961: The effect of the earth's surface on the S wave particle motion. *Bull. Seismol. Soc. Am.*, **51**, 237-246.

Peacock, S., S. Crampin, and D. C. Booth, 1988: Shear wave splitting in the Anzas eismic gap, southern California: temporal variation as possible precursors. *J. Geophys. Res.*, **93**, 3339-3356.

Savage, M. K., and P. G. Silver, 1990: Mantle anisotropy beneath western North America from teleseismic shear-wave splitting, EOS, Trans. Am. Geophys. Un., 71, 1442.

Shih, X. R., R. P. Meyer, and J. F. Schneider, 1989: An Automated, analytical method to determine shear-wave splitting. *Tectonophysics*, **165**, 271-278.

Shih, X. R., R. P. Meyer, and J. F. Schneider, 1991: Polarities of P and S wave, and shear wave splitting observed from the Bucaramanga Nest, Colombia. *J. Geopgys. Res.*, **96**, 12069-12082.

Zuniga, F. R., R. R. Castro, and T. Dominguez, 1995: Stress orientation and anisotropy based

on shear-wave splitting observations in the Cerro Prieto fault area, Baja California, Mexico. *PAGEOPH*, **144**, 39-57.